Int. J. Electrochem. Sci., 4 (**2009**) 1339 - 1350

International Journal of ELECTROCHEMICAL SCIENCE
www.electrochemsci.org

Study of 2-butyne-1,4-diol as Acid Corrosion Inhibitor for Mild Steel with Electrochemical, Infrared and AFM Techniques

M. G. Hosseini [1,*], *M. R. Arshadi* [2]

[1] Electrochemistry Research Laboratory, Department of Physical Chemistry, Chemistry Faculty, University of Tabriz, Tabriz, Iran
[2] Department of Physical Chemistry, Chemistry Faculty, Sharif University of Technology, Tehran, Iran
[*]E-mail: mg-hosseini@tabrizu.ac.ir

Received: 3 August 2009 / *Accepted:* 15 September 2009 / *Published:* 30 September 2009

The inhibition of mild steel corrosion in 0.5 M sulphuric acid by the symmetrical acetylenic alcohol 2-butyne-1,4-diol is investigated. Weight loss and electrochemical impedance data consistently indicate inhibition efficiencies up to 98%. Short-term impedance measurements reveal that the interfacial inhibition is a function of the exposure time, and that full performance is achieved faster as inhibitor concentration and temperature are higher. An infrared study of the surface film provides evidence that the film does not achieve its final state but after several hours. Atomic force Microscopy has been used for investigation the surface topography of metallic electrode.

Keywords: acetylenic alcohols, 2-butyne-1,4-diol, PMIRRAS, AFM

1. INTRODUCTION

Acid solutions are widely used in industry, the most important fields of application being acid pickling, industrial acid cleaning, acid descaling and oil well acidification [1-5]. Corrosion inhibitors are extremely used in industry to prevent or reduce the corrosion rates of metallic materials in these acid media. A considerable number of acetylenic compounds have been known for many decades as outstanding inhibitors of transition metal corrosion in acid solutions. The inhibitive performance, however, cannot be generalised, as several inhibitors have only moderate or poor suppressing effects on corrosion [6-7].

In an early study of acetylenic inhibitors [8], it was concluded that symmetrical compounds have poor inhibitive properties. Results obtained by the present authors, however, indicate that high inhibition efficiencies can be obtained with symmetrical acetylenic compounds. The study of the interaction of acetylenic compounds with iron and steel electrodes in aqueous acid solutions has received increasing interest in respect to the development of efficient corrosion inhibitors. Their effectiveness has been interpreted as due to chemisorptions and subsequent polymerization leading to the formation of barrier-type protective layers. The mechanism of the adsorption of these molecules and structures of the polymeric layers formed are not yet understood. Data available for comparison are limited as most published results refer to hydrochloric acid solutions, in which the acetylenic inhibitor is believed to benefit especially from the presence of specifically adsorbed chloride ions [9]. A different mechanism for the inhibition in sulphuric acid media can thus be anticipated.

Specially, the inhibition of propargyl alcohol (PA), one of the acetylenic alcohols, has been investigated extensively [10-16]. The decisive role of triple bonds of acetylenic alcohol molecules due to the p-electrons interaction with the metallic surfaces is generally accepted. Recently the inhibition properties of 2-butyn-1-ol, on the austenitic chromium–nickel surface [16] and 2-butyne 1-4 diol [11-14 , 17] on mild steel in sulfuric acid solutions have been investigated.

In this work, the inhibitive properties of the acetylenic alcohol 2-butyne-1, 4-diol (BD) are investigated for mild steel corrosion in sulphuric acid solution. Corrosion rate data from weight loss and electrochemical impedance measurements are combined with infrared observations of the surface film. Atomic force Microscopy has been used for investigation of the surface topography of metallic electrode.

2. EXPERIMENTAL PART

2.1. Materials

For weight loss measurements, mild steel specimens with the composition (in weight%) C 0.01, Si 0.35, P 0.018, Cr 0.04, Mo 0.03, Ni 0.017, Cu 0.02, Al 0.06 and Fe (balance) and dimensions 1×15×15 mm were used. The samples were polished to mirror finish using emery paper followed by aqueous alumina suspensions with particle sizes decreasing down to 0.05 μm, degreased by sonication in analytical reagent grade ethanol, and blown dry with nitrogen. Perfectly uniform wetability with water after this treatment was considered as a good indication for surface cleanliness. For electrochemical impedance studies, the metal was embedded in epoxy resin to expose a geometrical surface area of 1 cm^2 to the electrolyte. Prior to these measurements, the exposed surface was pretreated in the same manner as for weight loss experiments. All experiments were carried out under thermostatic conditions between 25 and 50 ºC (± 0.5 ºC), while the electrolyte solutions being in equilibrium with the atmosphere (*i.e.* aerated solutions). All purchased chemicals were of reagent grade (Merck, Aldrich) used without further purification, and twice-distilled water was used throughout.

2.2. Weight loss measurements

Gravimetric corrosion measurements were carried out according to the ASTM standard procedure described in [18]. In brief, mild steel specimens in triplicate were immersed for 6 hours in 100 mL H_2SO_4 0.5 M containing various concentrations of BD. Owing to the high inhibition efficiencies encountered, a shorter exposure did not allow differentiation between the different cases. The mass of the specimens before and after immersion was determined using an analytical balance accurate to 0.1 mg. In the present study, for the specified experimental conditions, relative differences between replicate experiments were found to be smaller than 5%, indicating good reproducibility. For further data processing, the average of the three replicate values was used.

2.3. Electrochemical impedance

Impedance measurements were carried out at the open circuit potential (E_{ocp}), using a computer-controlled potentiostat (PAR EG&G Model 273A) and frequency response analyser (Solartron Model 1255). In the conventional three-electrode assembly, a Pt foil auxiliary electrode and a saturated calomel reference electrode (SCE) were used.

During preliminary experiments, it was observed that immersion time had a pronounced effect on the obtained impedance spectra, suggesting that the structure of the inhibited metal|electrolyte interface reaches a steady state only after a certain time. Furthermore, the complex plane (Nyquist) diagrams obtained in the presence of BD had a simple semicircular shape, allowing straightforward modelling to a simplified Ershler-Randles equivalent circuit. Both considerations are sufficient arguments to carry out short-term impedance measurements, as introduced by Mertens and Temmerman for the study of developing passivating layers on metal surfaces [19]. In the present case, optimal measuring conditions were met by choosing 13 frequencies, logarithmically spaced between 1 and 10^4 Hz, allowing the registration of a spectrum in only about 25 s. A 5 mV peak-to-peak sine wave was employed as the excitation signal.

2.4. Infrared measurements

Fig. 1 shows the schematic set-up for the polarisation modulation infrared reflection absorption spectroscopy (PM-IRRAS). An FT-IR spectrometer with an evacuable bench (Bruker IFS 66/S) and a liquid nitrogen cooled mercury cadmium telluride (MCT) detector were used for these experiments. PM-IRRAS is ideally suited for recording the spectra of thin films on reflective substrates, but has been used seldom in the corrosion field [20, 21]. In this technique, the polarisation of the IR light is modulated between the s- and p-states at a frequency much higher (typically 100 kHz) than the Fourier frequencies. The differential absorption of s- and p-polarised IR radiation by the thin film on the surface is “coded” at this frequency. A phase-sensitive detector, locked onto the polarisation modulation frequency, directly yields the differential absorption of p- and s-polarised light by the surface layer. The much lower Fourier frequency signals from the interferometer gave the background single-beam spectrum. The PM-IRRAS spectrum is then calculated as the ratio of both.

Highly reflective iron surfaces were exposed to 0.5 M H_2SO_4 + 5 mM BD for time lenghtes ranging between 0.5 and 24 hours. Subsequently, the surfaces were rinsed with water and dried in air, after which the samples were mounted in the PM-IRRAS instrument. Interestingly, we found that PM-IRRAS can also be used to obtain a high quality IR spectrum for the bulk BD. For this purpose, a droplet of a saturated ethanolic solution of BD was placed on a gold-coated glass slide and allowed to dry, forming a thick film of bulk BD.

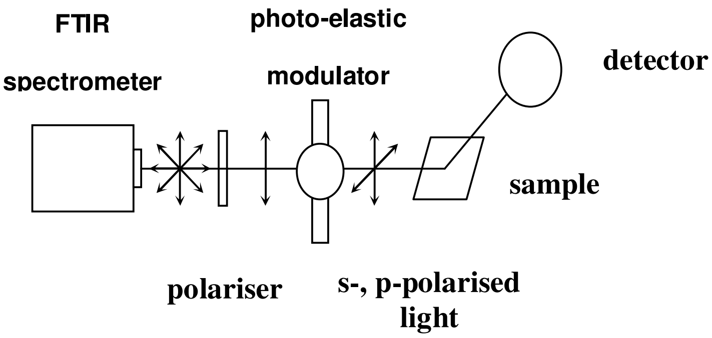

Figure 1. PM-IRRAS set-up

2.5. AFM measurement

AFM experiments were performed in the standard mode with a commercial AFM Instrument, Molecular Image (Pico Scan). Micro-fabricated Si_3N_4 pyramidal cantilevers (120 micrometer in length) with integrated Si_3N_4 Tips (20-50 nm radius of curvature) were used. The sparing constant of the cantilevers was 0.58 Nm^{-1} and the typical force during the measurements was less than 1 nm. First, the sample of Mild steel was mechanically polished with successively finer grades of SIC abrasive paper up to 4000 grade. Then washed with distilled water and acetone after immersion in 1M H_2SO_4 with and without addition of BD at room temperature for different immersion time, the specimen was cleaned with distilled water , dried with a cold air blaster , and then used for AFM measurements.

3. RESULTS AND DISCUSSION

3.1. Weight loss measurements

From the experimental weight loss data, percentage inhibition efficiencies $\eta_{\%w}$ was calculated in the classical way as follows:

$$\eta_{\%w} = \frac{W_0 - W}{W_0} \times 100 \tag{1}$$

where W_0 and W are the weight loss observed in the absence, and presence of the inhibitor, respectively. Values of $\eta_{\%w}$ for all investigated concentrations of BD in 0.5 M H_2SO_4 at temperatures between 25 and 50 ℃ were summarised in Table 1.

Table 1. Percentage inhibition efficiencies $\eta_{\%\mathrm{w}}$ from weight loss measurements

Table 1.

T (°C)	**c_{BD} (mM)**			
	0.1	**0.5**	**1.0**	**5.0**
25	50.0	91.3	96.2	98.2
30	58.5	92.4	97.5	97.1
40	73.0	93.5	95.2	96.8
45	76.0	88.0	96.0	96.1
50	84.0	83.0	93.5	95.0

For BD concentrations between 0.5 and 5 mM, efficiencies up to 98% and not less than 83% are observed at all investigated temperatures. Further, it is observed that with increasing temperature, a decrease in efficiency occurs, though not very pronounced. These results indicate that, conversely from what is claimed in [21], considerable inhibition efficiencies can be realised using symmetrical acetylenic compounds. The $\eta_{\%\mathrm{w}}\,(T)$-behaviour is commonly observed with inhibitors that act through adsorption at the metal|electrolyte interface.

More peculiar is the behaviour found for the lowest inhibitor concentration considered here (c_{BD} = 0.1 mM), for which an inverse variation of $\eta_{\%\mathrm{w}}$ with temperature is observed. Although it is somewhat premature to try and explain this finding based on the information available at this point, this observation seems to suggest that a number of competing processes take place on the iron surface.

The weight loss experiments being carried out over a period of 6 hours, the inhibition efficiencies in Table 1 necessarily represent average values over this period. To allow more instantaneous corrosion rate determinations, and to support the weight loss data, short-term impedance measurements were carried out.

3.2. Electrochemical impedance

Inhibition efficiencies $\eta_{\%\mathrm{Z}}$ in the present case was calculated through the following expression:

$$\eta_{\%\mathrm{Z}} = \frac{R_{\mathrm{ct0}}^{-1} - R_{\mathrm{ct}}^{-1}}{R_{\mathrm{ct0}}^{-1}} \times 100 = \frac{R_{\mathrm{ct}} - R_{\mathrm{ct0}}}{R_{\mathrm{ct}}} \times 100 \tag{2}$$

where R_{ct0} and R_{ct} are values of the charge transfer resistance [Ω m^2] observed in absence and presence of inhibitor, respectively. The values of R_{ct} were obtained from short-term impedance measurements, which were carried out during a period of one hour [19]. R_{ct0} was determined as soon as E_{ocp} reached a stable value (after about10 min). Longer delays in the uninhibited case led to decreasing values of the charge transfer resistance, which can logically be ascribed to an equivalent increase of true electrode surface area following a roughness increase due to the ongoing corrosion.

Fig. 2 shows the evolution of R_{ct} during the first hour of immersion, whereas Fig. 3 presents the corresponding evolution of the inhibition efficiency, calculated from Eqn. 2. For the three highest BD-concentrations, very similar patterns in $R_{ct}(t)$ are observed, although obviously the numerical values differ largely between the different cases. In each of these diagrams, R_{ct} sets off at a relatively low value (possibly a single characteristic value per concentration), after which an increase towards a stable value takes place. As the temperature is higher, the difference between the initial and final R_{ct}-values decreases.

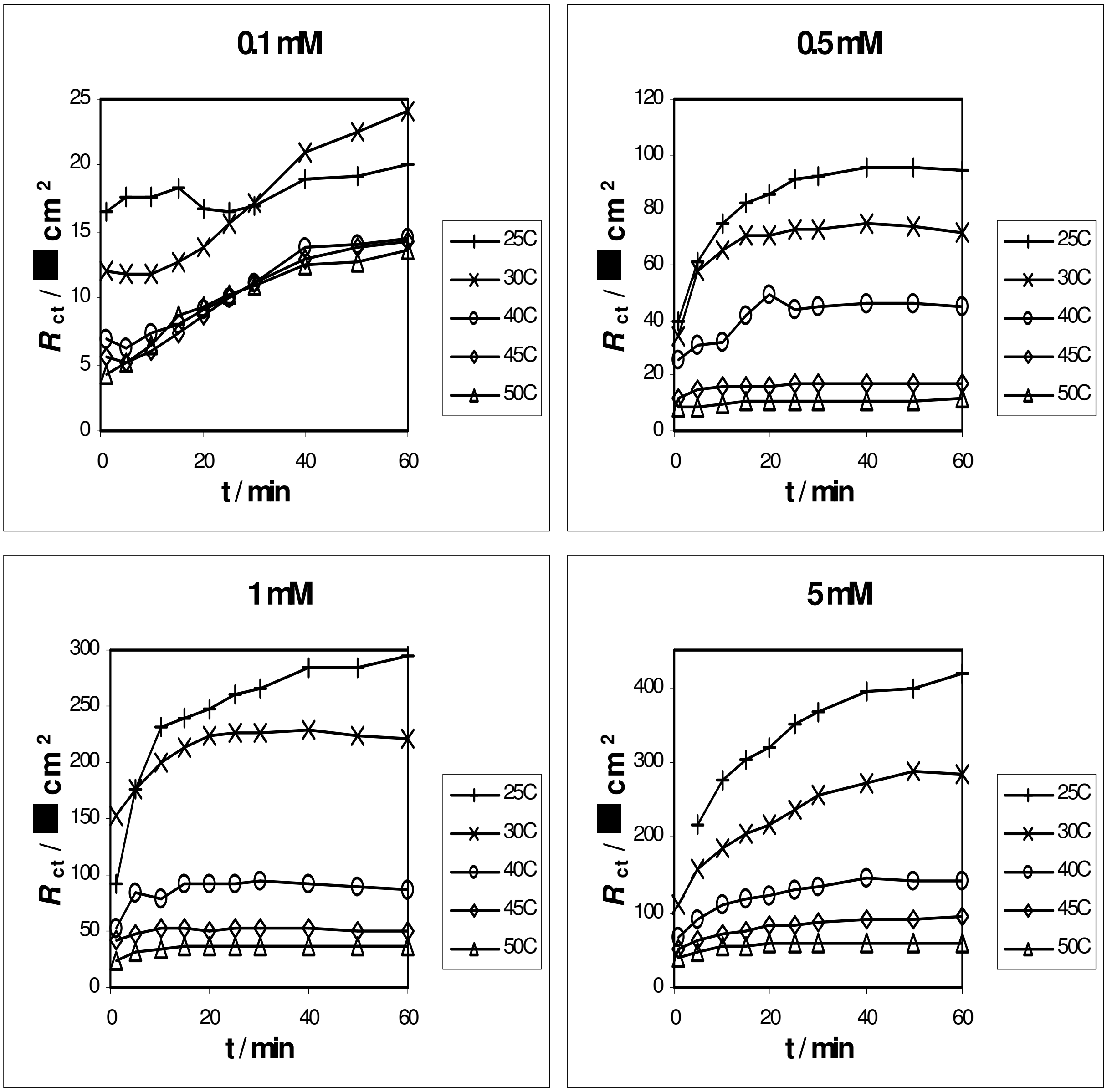

Figure 2. Evolution of charge transfer resistance upon immersion of mild steel in 0.5 M H_2SO_4 + x mM BD, at different temperatures

For the lowest concentration, again a different behaviour is observed. The increase of R_{ct} does not take place until a certain delay, and at 25 ºC, not considerable evolution occurs during the experiment. From Fig. 3, it is also clear that the impedance data confirm all observations that were based on the weight loss measurements, in the previous paragraph.

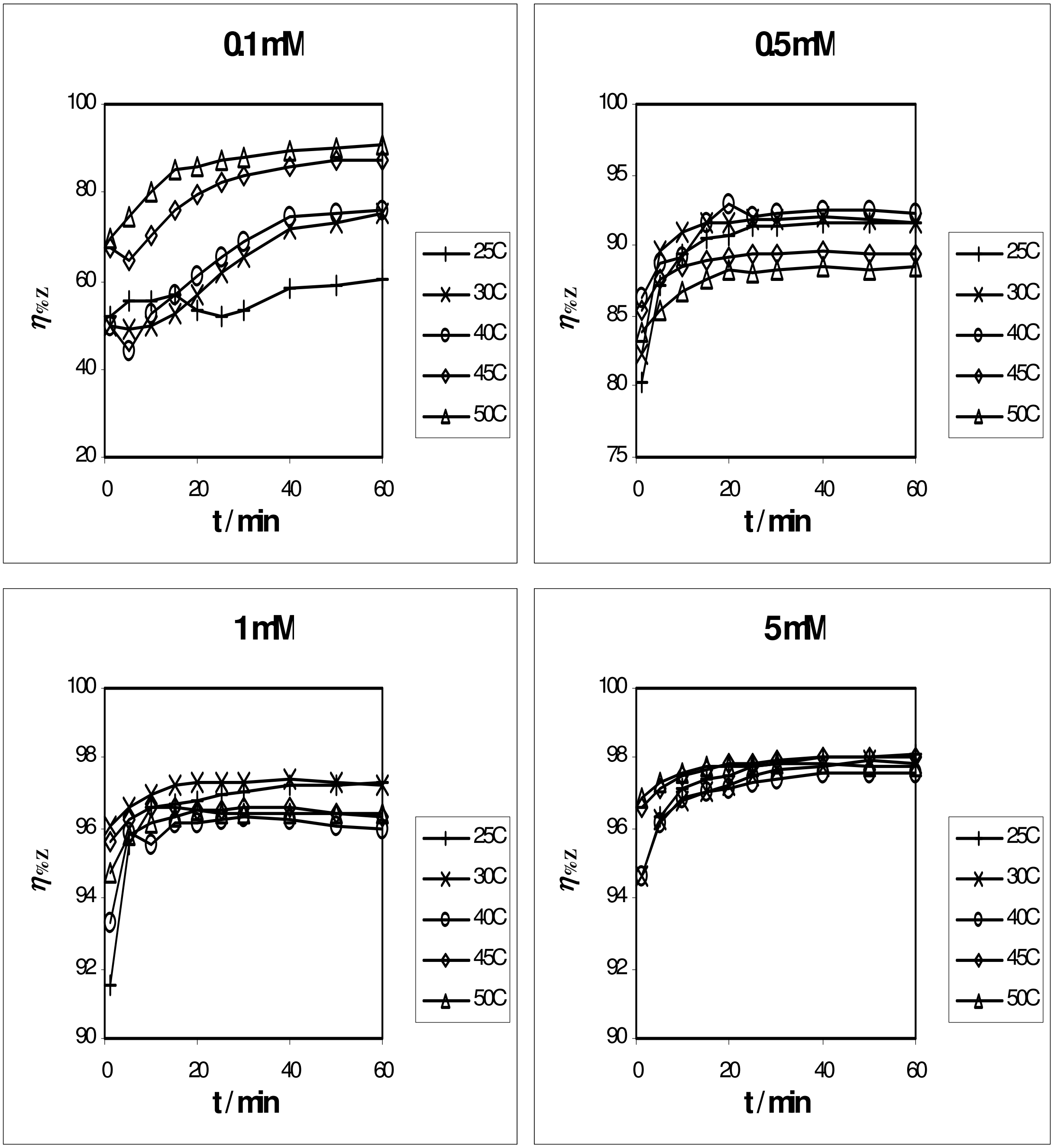

Figure 3. Evolution of corrosion inhibition efficiency upon immersion of mild steel in 0.5 M H_2SO_4 + *x* mM BD, at different temperatures

Fig. 2 shows a typical set of complex plane plots of mild steel in 0.5M H_2SO_4 in the absence and presence of various concentrations of the BD .In these spectra, variation of

Impedance response of mild steel after addition of the 2-BD to the acid media is remarkable. Increasing the concentration of the inhibitor caused the values of charge transfer resistance to shift to elevated amounts and this trend is truthful for the three studied Schiff bases.

Fig.3 shows Bode plots of mild steel in 0.5M H_2SO_4 containing different concentrations of BD. Occurrence of one inflexion point in the Bode plots indicated that there was one time constant in the corrosion reaction. The small deviations of phase angle from 90 and of the slope in the impedance modulus plot from 1 expresses that the system did not behave like an ideal capacitor.

3.3. PM-IRRAS

The PM-IRRAS spectrum for bulk BD is shown in Fig. 4a. Fig. 4b shows the spectra of the film formed on a mirroring mild steel surface after 30 minutes, 1.5 and 24 hours of exposure to 0.5 M sulphuric acid containing 5 mM BD. No reflection-absorption bands are observed after 30 minutes immersion. Exposure for 1.5 hours shows the gradual emergence of spectral features, resulting in clear absorption peaks after 24 hours.

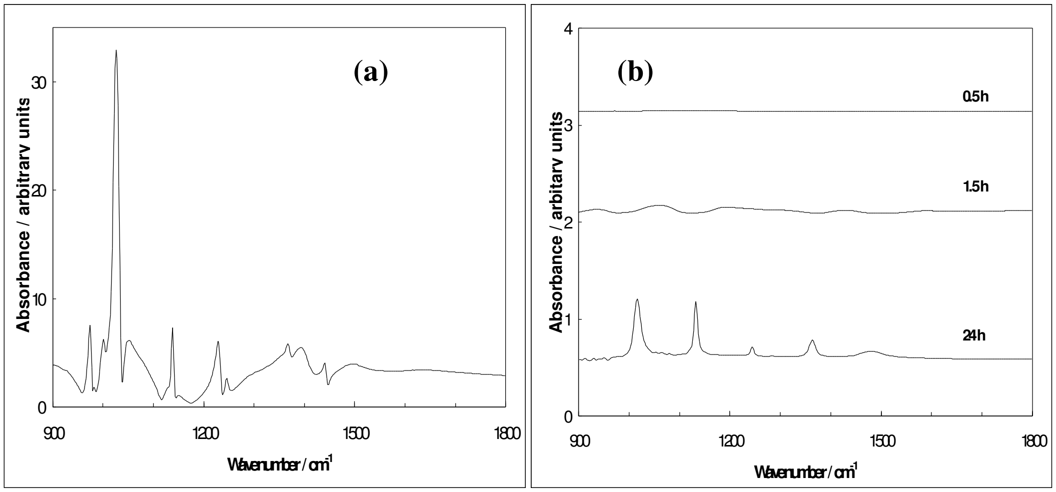

Figure 4. PM-IRRAS spectra for (a) bulk BD and (b) the surface film on mild steel after exposure to 0.5 M H_2SO_4 + 5 mM BD for times up to 24 h

Comparison of the spectrum after 24 hours of exposure with the bulk BD spectrum reveals a close similarity, as mostly differences in relative band intensities seem to occur. The most prominent IR absorptions for the surface film on iron are found at wave numbers around 1015 (C-O) and 1240-1360-1470 (CH_2) cm^{-1} [22]. Bands characteristic for acetylenic groups (expected around 3290, 2120 and 645 cm^{-1}) were not observed on the iron surface, but were rather faint in the bulk BD spectrum anyhow. The relatively strong band around 1130 cm^{-1} may well be caused by sulphate ions, either specifically adsorbed on the surface or as a ferrous/ferric precipitate.

An important deduction from the infrared behaviour as a function of exposure time is that apparently, the surface film requires much more than one hour to reach a stationary state, as suggested by the electrochemical data presented above. Several explanations can be formulated, but further experiments, which will include ellipsometry and multiple reflectances FT-IR, are required to settle the matter.

A first possibility is that a compact interfacial layer is formed relatively quickly, which largely determines the impedance behaviour (through the electrochemically active surface area). A further slow growth of a much more porous layer would then be much more obvious from a spectroscopic observation than from the electrochemical behaviour. A more detailed analysis of impedance data should reveal this if applicable, as can theoretically be shown [23].

A second possibility is that the surface layer is indeed formed within the first hour of metal exposure, but that the molecular orientation or the bonding within the layer is such that no efficient interaction with the infrared light occurs. Upon increasing exposure, a slow rearrangement may take place within the surface layer, now resulting in a more IR-active film, but not necessarily affecting the electrochemical features.

3.4. AFM

The atomic force microscopy (AFM) provides a powerful means of characterization the microstructure [24-25]. Fig.5 and Fig.6a show the surface structure image of mild steel in 0.5 mol L^{-1} H_2SO_4 solution with 5 min immersion time and in the present of 10 mmol BD with 30 min immersion respectively. Fig. 6b illustrates the corresponding three dimensionall AFM images. As can be seen from this Fig.5, the corrosion of mild steel samples in the absence of inhibitor appeared relatively uniform in general and some part to a low-mound-like structure. The image is quite different from the pitting corrosion image [26].

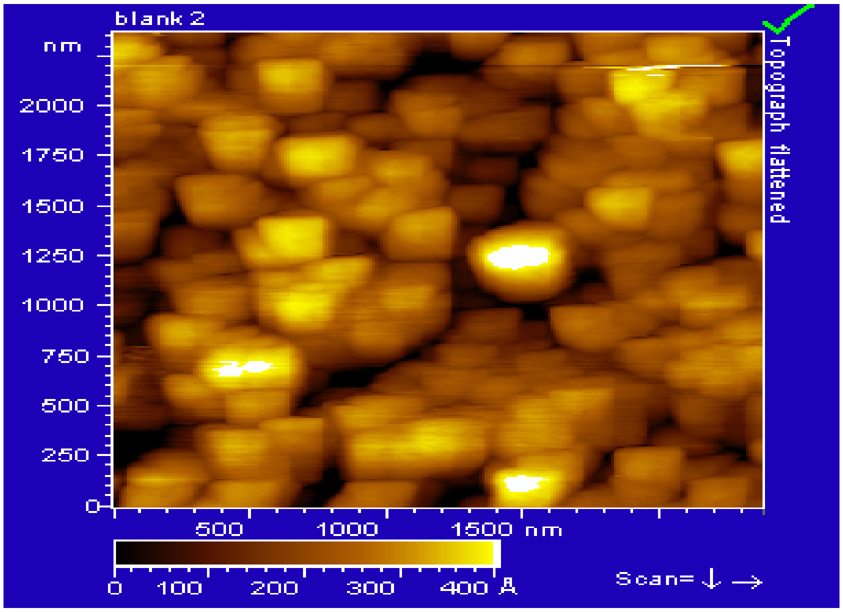

Figure 5. AFM images of surface topography in 0.5 M H_2SO_4 in the absence of BD after 10 min. immersion time

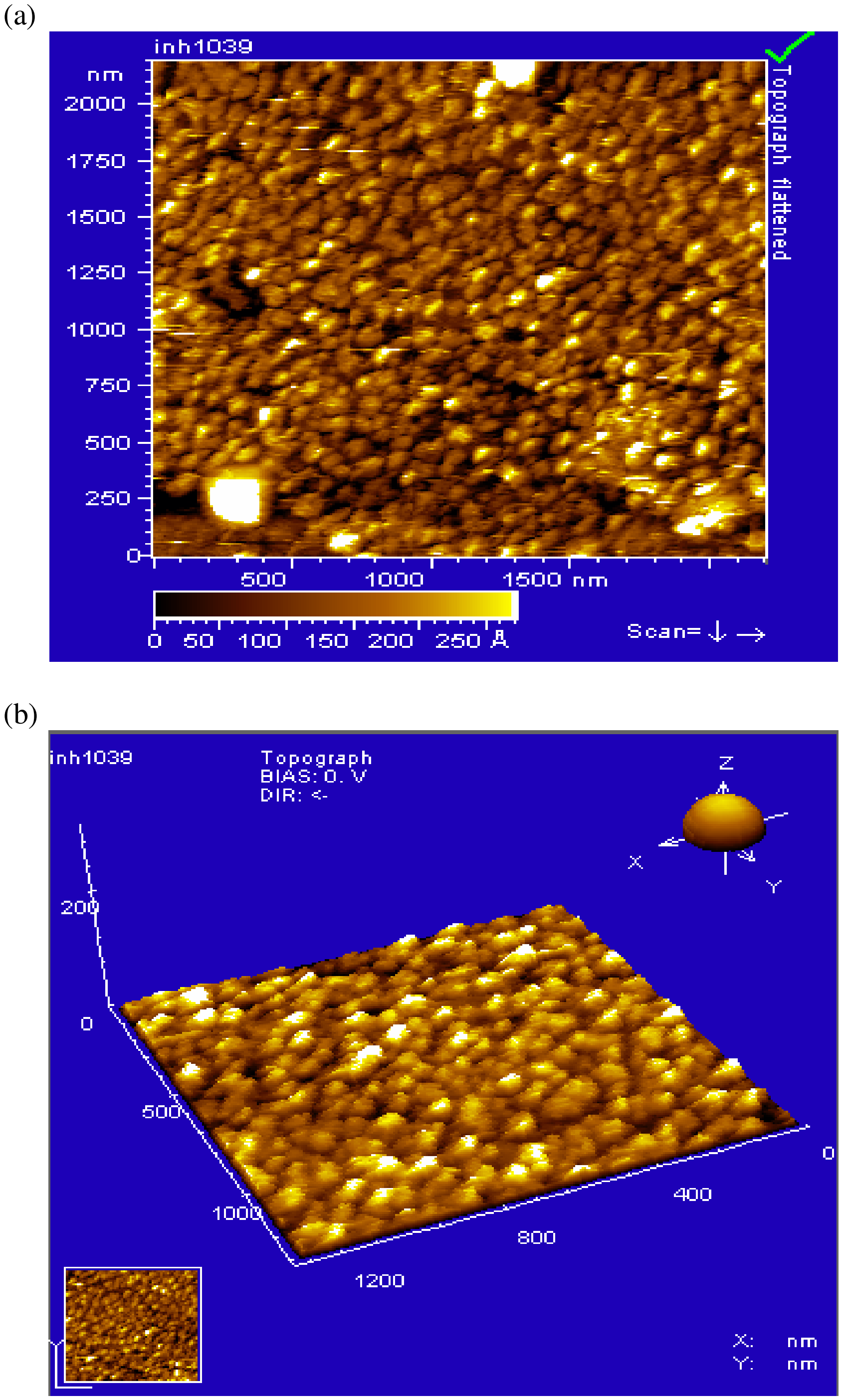

Figure 6. a) AFM images of surface topography in 0.5 M H_2SO_4 in the presence of 10 mmole BD after 30 min immersion time. b) The corresponding three dimension AFM images.

However, in the presence of 10 mmole BD, the surface becomes more flat and compact. Also the analysis of data in f Fig. 6 shows that the layer height values approximately are 200 and 100 nm, respectively Thus the corrosion of mild steel decreases after adding BD in H_2SO_4.

In the presence of BD, the surface porosity and the corrosion rate are very lower than those in the absence of BD. This is due to adsorption of the BD on the surface, so the roughness of surface very low. Comparison of Fig. 5 and 6 clearly shows that the corrosion degrees of mild steel decreases in the presence of BD. Fig. 6 shows the spherical or bread-like particle appearance on the surfaces, which do not exist in the Fig.5. Therefore, it may be concluded that these particles are the adsorption film of the inhibitor BD which efficiently inhibits the corrosion of mild steel. These results have been supported via PM-IRRS experiments on Fe corrosion in sulphuric acid and in the presence of BD which showed that in the H_2SO_4, the Fe atoms are irreversibly moved out by a simple dissolution into the acidic electrolyte and a more complex dissolution precipitation mechanism leads to pitting corrosion. Conversely, the inhibiting media (BD) are characterized by low surface changes, so the atoms are weakly displaced and the oxidation–reduction phenomenon is reversible, on the other hand, B.D has been identified as an inhibitor by precipitation mechanism leading to the formation of thin passive deposit on the metallic surface

As a consequence, further investigations are in progress in order to improve the quality and resolution of AFM images by developing new polishing procedures or by working on mono crystalline substrates.

4. CONCLUSIONS

The inhibitive performance of 2-butyne-1,4-diol (BD) on the sulphuric acid corrosion of mild steel was determined by weight loss and electrochemical impedance measurements. It was found that inhibition efficiencies upto 98 % could be obtained, identifying the considered diol as quite an effective inhibitor. The introduction of BD into 0.5M H2SO4 solution results in the formation of a thin inhibitor film on the mild steel surface, which causes the decrease surface roughness and effectively protects mild steel from corrosion.

Short-term impedance data indicate that on the level of the metal|electrolyte interface, a steady state is reached within the first hour of the metal exposure to BD-inhibited 0.5 M sulphuric acid. PM-IRRAS data, on the other hand, suggest that the film formation on the metal surface is a slow process, and that a steady state is not achieved until several hours after immersion. Both findings may be reconciled by assuming the metal-film interface reaches its final structure fast, and that growth of a much more porous over layer continues for much longer. Alternatively, a slow rearrangement within the surface layer, yielding a more IR-active film, may explain these observations.

ACKNOWLEDGEMENTS
The Author gratefully acknowledges the member of Richard Nichols SPM laboratory in Liverpool University and warmly appreciates the assistance of Dr. S.F.L. Merten (Belgium).

References

1. M.G. Hosseini, M. Ehteshamzadeh, T. Shahrabi, *Electrochim. Acta, 52* (2007) 3580.
2. M.G. Hosseini, S.F.L. Mertens, M. Ghorbani, M.R. Arshadi, *Mater. Chem. Phys*, 78 (2003) 800.

3. H.B. Fan, C.Y. Fu, H.L. Wang, X.P. Guo, J.S. Zheng, *Br. Corros. J.* 37 (2002) 122.
4. M.G. Hosseini, S.F.L. Mertens, M.R. Arshadi, *Corros. Sci.* 45 (2003) 1473.
5. M.G. Hosseini, T. Shahrabi, H .Tavakholi, *Anti-Corrosn Methods and Materials*; 54 (2007) 147
6. M.R. Arshadi, M.G. Hosseini, M.R. Ghorbani, *Br. Corros. J.* 37 (2002) 76.
7. M. Ehteshamzadeh, T. Shahrabi, M.G. Hosseini, *Appl. Surf. Sci*. 252 (2006) 949.
8. G.L. Foster, B.D. Oakes, C.H. Kucera, *Ind. Eng. Chem*. 51 (1959) 825.
9. F.B. Growcock, V.R.Lopp, *Corros. Sci*. 28 (1988)397.
10. R.J. Tedeschi, *Corrosion* 31 (1975) 130.
11. A.R. Yazdzad, T.Shahrabi, M.G. Hosseini, *Mat. Chem. Phy* 109 (2008) 199.
12. T. Shahrabi, A.R. Yazdzad, M.G. Hosseini *J. Mat. Sci. Tech*. 24 (2008) 427.
13. M.G. Hosseini, T.Shahrabi, H. Tavakholi, *J. Appl. Elec*. 38 (2008) 1629.
14. B. Paty, D.D. Singh, *Corros*. 48 (1992) 442.
15. Bartos, Hackerman, M. N. *J. Electrochem. Soc*. 34 (1992) 28 .
16. BilgiçS. Sahin M.¸ (2001), *Mat. Chem. Phy*. 70 :290.
17. M.G. Hosseini, S. F.L. Mertens, R.J. Nichols, M.Ghorbani, M.R. Arshadi, Eurocorr 2002, 24Sep., Madrid Spain.
18. ASTM, *Standard practice for laboratory immersion corrosion testing of metals,* G 31–72, Philadelphia, PA, 1990, p. 401.
19. S.F.L. Mertens, E. Temmerman, *Corros. Sci.* 43 (2001) 301.
20. Chen P., Smith M.J., Garland B., *American Laboratory,* Nov. 2000, p.36.
21. B.L. Frey, R.M. Corn, *Anal. Chem.* 68 (1996) 3187.
22. G.W. Poling, *J. Electrochem. Soc.* 114 (1967) 1209.
23. S.F.L. Mertens, E. Temmerman, *ACH-Models in Chem*. 137 (2000) 95.
24. A.A. Gewirth, B.K. Niece, *Chem. Rev*. 97 (1997) 1129.
25. J. Li, D. Lampner, *Colloids Surf.* A 154 (1999) 227.
26. Abd El Rehim S.S., Hassaan H.H. and Amin M.A. (2002), *Mat. Chem. Phys*. 783:37.